Capacity Analysis of Multihop ORS-Assisted FSO Communication Systems

End Semester Evaluation 2024

Presented by

Deepak Jaladi

B.Tech (210002039), Communication & Signal Processing (CSP)

Supervisor

Dr. Swaminathan Ramabadran

Department of Electrical Engineering

Indian Institute of Technology Indore

Table of Contents

FSO communication and its advantages

Free-Space Optical (FSO) Communication refers to the transmission of data through a free space medium (such as air, outer space, or vacuum) using optical signals, typically laser beams. It serves as an alternative to fiber-optic communication, without the need for physical cables. The data is transmitted as light beams modulated to carry information between two points.

- **High Bandwidth:** FSO offers high data rates, making it suitable for applications requiring fast communication.
- **Cost-Effective:** No need for expensive infrastructure like fiber cables; installation is quick and affordable.
- **Ease of Deployment**: Can be rapidly deployed, especially in areas where laying cables is challenging (e.g., mountains, urban settings).
- **No Spectrum Licensing:** Operates in unlicensed optical wavelengths, avoiding regulatory constraints.
- **Low Latency:** Provides faster communication compared to some traditional wireless technologies.

IRS and ORS

Intelligent Reflecting Surface (IRS) is a passive array of programmable reflecting elements that can manipulate the phase, amplitude, and polarization of incident electromagnetic waves to enhance communication links.

Table 1: FSO vs RF IRS design

Properties	**FSO**	**RF**
Wavelength	Shorter wavelengths, necessitate precise and highly sensitive surface designs.	Longer wavelengths, requiring less precision
Material and Structure	Uses micro-mirrors, liquid crystals, or metasurfaces	Employs electronically tunable materials like varactors or PIN diodes
Sensitivity	Highly sensitive to misalignment due to the narrow laser beams	Less alignment-sensitive because of broader RF wave propagation and diffraction characteristics
Environmental Factors	Needs to address challenges like atmospheric turbulence, fog, and scattering that significantly affect optical signals	Must deal with different environmental effects such as multipath fading and electromagnetic interference, but is less affected by weather conditions

where ORS is a special case of optical RIS when it operates as a perfect mirror, it is mandatory to consider multiple ORSs between source and destination in a backhaul network scenario.

Proposed System Model

Multihop FSO communication involves relaying data through multiple intermediate hops rather than establishing a single long-distance direct link. We use decode-and-forward (DF) relaying in this model.

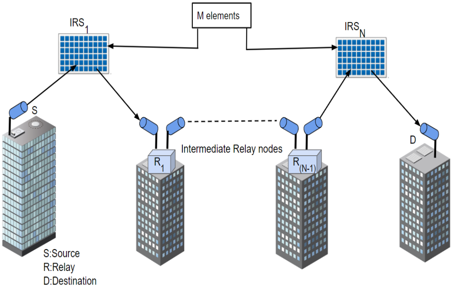

Fig. 1: IRS-Assisted multihop FSO System

- **Improved Signal Quality:** Splitting the path into shorter hops reduces attenuation, scattering, and turbulence effects.
- **Extended Coverage:** Multihop networks can cover longer distances by using intermediate relay hops, bypassing the limitations of a single-link system.
- **Reliability:** Shorter hops are less sensitive to environmental factors like fog, rain, or dust, making the overall system more robust to adverse weather conditions.
- **Reduced Beam Divergence:** Over shorter distances, the optical beam remains narrow, minimizing power loss and improving receiver alignment.

Problem Statement: Capacity Analysis of Multihop ORS-Assisted FSO Communication Systems

- Closed-form expressions of ergodic capacity (EC) were derived without invoking the central limit theorem (CLT)
- The effect of atmospheric turbulence (AT), pointing errors, and fog were considered in the numerical results
- Expressions of EC are derived for different statistical models of AT (i.e., Gamma-Gamma, Málaga and IGGG distributions)
- We conduct Monte-Carlo simulations to verify the correctness of derived analytical expressions
- This model performed better than the free space optics (FSO) system without the ORS

Literature Review and Motivations

Table 2: Literature Review

Reference	Type of system	Link Distribution	Metrics
[1]	Dual-hop (DH) FSO	Gamma-Gamma	ABER, OP and EC
[2]	DH FSO/RF	FSO—Gamma—Gamma, RF—Nakagami—m	ABER, OP and EC
[3]	Multihop FSO	Gamma—Gamma	OP
[4]	DH IRS—assisted FSO/RF	FSO—Gamma—Gamma, RF—Rayleigh	ABER, OP
[5]	Multihop IRS—assisted FSO	FSO—Gamma—Gamma, Málaga, IGGG	ABER, OP
This model	Multihop ORS—assisted FSO	FSO—Gamma—Gamma, Málaga, IGGG	EC

Motivations

- Using ORS in each hop improves the coverage and this sort of model is proposed keeping in mind the dense urban environment
- There is less amount of work done on ORS-assisted multihop FSO communication, where ORS in each hop is enabled to enable LoS communication

System Model

- The overall channel coefficient for p^{th} hop, Z_p can be written as $Z_p = h_1^{(p)} h_2^{(p)}$, where $h_i^{(p)} = h_{a_i}^{(p)} h_{pe_i}^{(p)} h_{f_i}^{(p)}$ of any p^{th} hop and the received FSO signal at the photodetector of any p^{th} hop is given as [**5**, **Eq.1**]

$$y_p = Z_p x_p + n_p$$

  - x_p is the message signal transmitted from Tx and n_p is the AWGN with zero-mean and variance $\sigma_{o_p}^2$ for any p^{th} hop

- The PDF of pointing error coefficient, h_{pe} is given as [**5**, **Eq.6**]

$$f_{h_{pe}}^{(p)}(x) = \frac{(g^{(p)})^2}{A_0} \left(\frac{x}{A_0} \right)^{(g^{(p)})^2 - 1}$$

- The PDF of fog fading coefficient, $h_f^{(p)}$ is given as [**5**, **Eq.7**]

$$f_{h_f}^{(p)}(x) = \frac{(v^{(p)})^{k^{(p)}}}{\Gamma(k^{(p)})} \left[ln \left(\frac{1}{x} \right) \right]^{k^{(p)} - 1} x^{v^{(p)} - 1}$$

  - A_0 is the power received when radial displacement, $r^{(p)} = 0$ and $g^{(p)}$ is the pointing error coefficient.
  - $v^{(p)} = \frac{4.343}{L^{(p)} \psi^{(p)}}$, $\psi^{(p)}$ is size parameter and $k^{(p)}$ is shape parameter.

Channel Model: Gamma−Gamma

- The probability density function (PDF) atmospheric turbulence from Tx to IRS of any p^{th} hop, $f_{h_a}^{(p)}$ is [**5**, **Eq.2**]

$$f_{h_a}^{(p)}(x) = \frac{2(\alpha^{(p)}\beta^{(p)})^{\frac{\alpha^{(p)}+\beta^{(p)}}{2}}}{\Gamma(\alpha^{(p)})\Gamma(\beta^{(p)})} x^{\frac{\alpha^{(p)}+\beta^{(p)}}{2}-1} K_{\alpha^{(p)}-\beta^{(p)}}(2\sqrt{\alpha^{(p)}\beta^{(p)}x})$$

  - $K_d(.)$ is the modified Bessel function of second kind and d^{th} order, $\alpha^{(p)}$ and $\beta^{(p)}$ are the large and small scale scattering parameters

- The PDF of the instantaneous SNR, $\gamma^{(p)}$ is given as

$$f_{\gamma^{(p)}}(\gamma) = \frac{1}{2\gamma}\left(\zeta_1^{(p)}\zeta_2^{(p)}\right)^{-1}\left(\chi_1^{(p)}\chi_2^{(p)}\right)\left((v_1^{(p)})^{k_1^{(p)}}(v_2^{(p)})^{k_2^{(p)}}\right)$$
$$G_{2+k_1^{(p)}+k_2^{(p)},\ 6+k_1^{(p)}+k_2^{(p)}}^{6+k_1^{(p)}+k_2^{(p)},\ 0}\left(\left((\zeta_1^{(p)}\zeta_2^{(p)})\sqrt{\frac{\gamma B^2}{\overline{\gamma^{(p)}}}}\right)\middle|\begin{matrix}\Delta_1\\ \Delta_2\end{matrix}\right)$$

  - $G_{p,q}^{m,n}(.)$ is Meijer's G-function, $\chi_i^{(p)} = \frac{\alpha_i^{(p)}\beta_i^{(p)}(g_i^{(p)})^2}{A_0\Gamma(\alpha_i^{(p)})\Gamma(\beta_i^{(p)})}$, $\zeta_i^{(p)} = \frac{\alpha_i^{(p)}\beta_i^{(p)}}{A_0}$ and $\gamma^{(p)} = \frac{\overline{\gamma^{(p)}}Z_p^2}{B^2}$
  - $\overline{\gamma^{(p)}}$ is the average electrical SNR and B is the expectation value of overall channel coefficient Z_p.

Channel Model: Málaga

- The probability density function (PDF) atmospheric turbulence from Tx to IRS of any p^{th} hop, $f_{h_a}^{(p)}$ is [**6**, **Eq.3**]

$$f_{h_a}^{(p)}(x) = A_M \sum_{d^{(p)}=1}^{\beta^{(p)}} a_d x^{\frac{\alpha^{(p)}+d^{(p)}}{2}-1} K_{\alpha^{(p)}-\beta^{(p)}} \left(2\sqrt{\frac{\alpha^{(p)}\beta^{(p)}x}{y^{(p)}\beta^{(p)}+\Omega'^{(p)}}} \right)$$

  - $A_M^{(p)} = \frac{2\alpha^{(p)}{}^{\alpha^{(p)}/2}}{y^{(p)}{}^{1+\alpha^{(p)}/2}\Gamma(\alpha^{(p)})} \left(\frac{y^{(p)}\beta^{(p)}}{y^{(p)}\beta^{(p)}+\Omega'^{(p)}} \right)^{\beta^{(p)}+\alpha^{(p)}/2}$ and
    $a_d^{(p)} = \begin{pmatrix} \beta^{(p)}-1 \\ d^{(p)}-1 \end{pmatrix} \frac{(y^{(p)}\beta^{(p)}+\Omega'^{(p)})^{1-d^{(p)}/2}}{(d^{(p)}-1)!} \left(\frac{\Omega'^{(p)}}{y^{(p)}} \right)^{d^{(p)}-1} \left(\frac{\alpha^{(p)}}{\beta^{(p)}} \right)^{d^{(p)}/2}$
  - $\Omega'^{(p)}$ and $y^{(p)}$ are parameters related to power of different components of Málaga distribution.

- The PDF of the instantaneous SNR, $\gamma^{(p)}$ is given as

$$f_{\gamma^{(p)}}(\gamma) = \frac{1}{2\gamma} \left(\zeta_1^{(p)} \zeta_2^{(p)} \right)^{-1} \left(\chi_1^{(p)} \chi_2^{(p)} \right) \left((v_1^{(p)})^{k_1^{(p)}} (v_2^{(p)})^{k_2^{(p)}} \right)$$

$$\sum_{d_1^{(p)}=1}^{\beta_1^{(p)}} \sum_{d_2^{(p)}=1}^{\beta_2^{(p)}} b_{d_1} b_{d_2} G^{6+k_1^{(p)}+k_2^{(p)} \quad 0}_{2+k_1^{(p)}+k_2^{(p)} \quad 6+k_1^{(p)}+k_2^{(p)}} \left(\left((\zeta_1^{(p)} \zeta_2^{(p)}) \sqrt{\frac{\gamma B^2}{\overline{\gamma}^{(p)}}} \right) \middle| \begin{matrix} \Delta_1 \\ \Delta_3 \end{matrix} \right)$$

  - $\chi_i^{(p)} = \frac{A_{M_i}^{(p)} \alpha_i^{(p)} \beta_i^{(p)} (g_i^{(p)})^2}{2A_0(y_i^{(p)}\beta_i^{(p)}+\Omega_i'^{(p)})}$ and $\zeta_i^{(p)} = \frac{\alpha_i^{(p)}\beta_i^{(p)}}{A_0(y_i^{(p)}\beta_i^{(p)}+\Omega_i'^{(p)})}$

Channel Model: IGGG

- The probability density function (PDF) atmospheric turbulence from Tx to IRS of any p^{th} hop, $f_{h_a}^{(p)}$ is [7]

$$f_{h_a}^{(p)}(x) = \frac{A}{x} G_{1\,2}^{2\,1}\left(\frac{\alpha^{(p)}\beta^{(p)}x}{\lambda^{(p)}-1} \middle| \begin{matrix} 1-\lambda^{(p)} \\ \alpha^{(p)}, \beta^{(p)} \end{matrix} \right)$$

  - $A = \frac{1}{\Gamma(\alpha^{(p)})\Gamma(\beta^{(p)})\Gamma(\lambda^{(p)})}$, $\alpha^{(p)}$, $\beta^{(p)}$ and $\lambda^{(p)} = \alpha^{(p)} + 2$ are the large, medium and small scale scattering parameters

- The PDF of the instantaneous SNR, $\gamma^{(p)}$ is given as

$$f_{\gamma^{(p)}}(\gamma) = \frac{1}{2\gamma}\left(\zeta_1^{(p)}\zeta_2^{(p)}\right)^{-1}\left(\chi_1^{(p)}\chi_2^{(p)}\right)\left((v_1^{(p)})^{k_1^{(p)}}(v_2^{(p)})^{k_2^{(p)}}\right)$$
$$G_{4+k_1^{(p)}+k_2^{(p)}\ \ 6+k_1^{(p)}+k_2^{(p)}}^{6+k_1^{(p)}+k_2^{(p)}\ \ 2}\left(\left((\zeta_1^{(p)}\zeta_2^{(p)})\sqrt{\frac{\gamma B^2}{\overline{\gamma^{(p)}}}}\right) \middle| \begin{matrix} \Delta_4 \\ \Delta_2 \end{matrix}\right)$$

  - $\chi_i^{(p)} = \frac{A_i^{(p)}\alpha_i^{(p)}\beta_i^{(p)}(g_i^{(p)})^2}{A_0(\lambda_i^{(p)}-1)}$ and $\zeta_i^{(p)} = \frac{\alpha_i^{(p)}\beta_i^{(p)}}{A_0(\lambda_i^{(p)}-1)}$

Multihop ORS-Assisted FSO: Performance Metrics

- The capacity of the p^{th} hop is derived by solving the integral

$$C^{(p)} = \int_0^{\infty} log_2(1 + s_r\gamma) f_{\gamma^{(p)}}$$

- According to the min-cut max-flow theorem, the system's overall capacity cannot be greater than the capacity of an individual hop. Therefore, the upper bound for the capacity is given as [**8**, **Eq.29**]

$$C_{DF} = min\left(C^{(1)}, C^{(2)}, \cdots, C^{(N)}\right)$$

- The Ergodic capacity of the proposed system model is derived as

$$C^{(p)} = \frac{2^{\alpha_1^{(p)}+\alpha_2^{(p)}+\beta_1^{(p)}+\beta_2^{(p)}-k_1^{(p)}-k_2^{(p)}-6}}{\pi^2 ln2} \left(\zeta_1^{(p)}\zeta_2^{(p)}\right)^{-1} \left(\chi_1^{(p)}\chi_2^{(p)}\right) \left((v_1^{(p)})^{k_1^{(p)}}(v_2^{(p)})^{k_2^{(p)}}\right)$$
$$G^{\,14+2k_1^{(p)}+2k_2^{(p)} \quad 1}_{\,6+2k_1^{(p)}+2k_2^{(p)} \quad 14+2k_1^{(p)}+2k_2^{(p)}} \left(\frac{(\zeta_1^{(p)}\zeta_2^{(p)})^2 B^2}{256 s_r \overline{\gamma^{(p)}}} \middle| \begin{matrix} \Delta_5 \\ \Delta_6 \end{matrix} \right)$$
$$(Gamma - Gamma)$$

$$C^{(p)} = \frac{\left(\zeta_1^{(p)}\zeta_2^{(p)}\right)^{-1}\left(\chi_1^{(p)}\chi_2^{(p)}\right)\left(\left(v_1^{(p)}\right)^{k_1^{(p)}}\left(v_2^{(p)}\right)^{k_2^{(p)}}\right)}{\pi^2 ln2} \sum_{d_1^{(p)}=1}^{\beta_1^{(p)}} \sum_{d_2^{(p)}=1}^{\beta_2^{(p)}} b_{d_1} b_{d_2}$$

$$2^{\alpha_1^{(p)}+\alpha_2^{(p)}+d_1^{(p)}+d_2^{(p)}-k_1^{(p)}-k_2^{(p)}-6} G^{14+2k_1^{(p)}+2k_2^{(p)},\ 1}_{6+2k_1^{(p)}+2k_2^{(p)},\ 14+2k_1^{(p)}+2k_2^{(p)}}\left(\frac{(\zeta_1^{(p)}\zeta_2^{(p)})^2 B^2}{256 s_r \overline{\gamma^{(p)}}}\middle|\begin{matrix}\Delta_5\\ \Delta_7\end{matrix}\right)$$

$$(Málaga)$$

$$C^{(p)} = \frac{2^{\alpha_1^{(p)}+\alpha_2^{(p)}+\beta_1^{(p)}+\beta_2^{(p)}+\lambda_1^{(p)}+\lambda_2^{(p)}-k_1^{(p)}-k_2^{(p)}-8}}{\pi^3 ln2}\left(\zeta_1^{(p)}\zeta_2^{(p)}\right)^{-1}\left(\chi_1^{(p)}\chi_2^{(p)}\right)$$

$$\left(\left(v_1^{(p)}\right)^{k_1^{(p)}}\left(v_2^{(p)}\right)^{k_2^{(p)}}\right) G^{14+2k_1^{(p)}+2k_2^{(p)},\ 5}_{10+2k_1^{(p)}+2k_2^{(p)},\ 14+2k_1^{(p)}+2k_2^{(p)}}\left(\frac{(\zeta_1^{(p)}\zeta_2^{(p)})^2 B^2}{16 s_r \overline{\gamma^{(p)}}}\middle|\begin{matrix}\Delta_8\\ \Delta_6\end{matrix}\right)$$

$$(IGGG)$$

Notations Used

Table 3: List of Notations

$\Delta_1 = 1 + (g_1^{(p)})^2, 1 + (g_2^{(p)})^2, \{1 + v_1^{(p)}\}_1^{k_1^{(p)}}, \{1 + v_2^{(p)}\}_1^{k_2^{(p)}}$
$\Delta_2 = (g_1^{(p)})^2, (g_2^{(p)})^2, \alpha_1^{(p)}, \alpha_2^{(p)}, \beta_1^{(p)}, \beta_2^{(p)}, \{v_1^{(p)}\}_1^{k_1^{(p)}}, \{v_2^{(p)}\}_1^{k_2^{(p)}}$
$\Delta_3 = (g_1^{(p)})^2, (g_2^{(p)})^2, \alpha_1^{(p)}, \alpha_2^{(p)}, d_1^{(p)}, d_2^{(p)}, \{v_1^{(p)}\}_1^{k_1^{(p)}}, \{v_2^{(p)}\}_1^{k_2^{(p)}}$
$\Delta_4 = 1 - \lambda_1^{(p)}, 1 - \lambda_2^{(p)}, 1 + (g_1^{(p)})^2, 1 + (g_2^{(p)})^2, \{1 + v_1^{(p)}\}_1^{k_1^{(p)}}, \{1 + v_2^{(p)}\}_1^{k_2^{(p)}}$
$\Delta_5 = 0, 1, \frac{1+(g_1^{(p)})^2}{2}, \frac{2+(g_1^{(p)})^2}{2}, \frac{1+(g_2^{(p)})^2}{2}, \frac{2+(g_2^{(p)})^2}{2}, \{\frac{1+v_1^{(p)}}{2}\}_1^{k_1^{(p)}}, \{\frac{2+v_1^{(p)}}{2}\}_1^{k_1^{(p)}}, \{\frac{1+v_2^{(p)}}{2}\}_1^{k_2^{(p)}}, \{\frac{2+v_2^{(p)}}{2}\}_1^{k_2^{(p)}}$
$\Delta_6 = \frac{(g_1^{(p)})^2}{2}, \frac{1+(g_1^{(p)})^2}{2}, \frac{(g_2^{(p)})^2}{2}, \frac{1+(g_2^{(p)})^2}{2}, \frac{\alpha_1^{(p)}}{2}, \frac{1+\alpha_1^{(p)}}{2}, \frac{\alpha_2^{(p)}}{2}, \frac{1+\alpha_2^{(p)}}{2}, \frac{\beta_1^{(p)}}{2}, \frac{1+\beta_1^{(p)}}{2}, \frac{\beta_2^{(p)}}{2}, \frac{1+\beta_2^{(p)}}{2},$ $\{\frac{v_1^{(p)}}{2}\}_1^{k_1^{(p)}}, \{\frac{1+v_1^{(p)}}{2}\}_1^{k_1^{(p)}}, \{\frac{v_2^{(p)}}{2}\}_1^{k_2^{(p)}}, \{\frac{1+v_2^{(p)}}{2}\}_1^{k_2^{(p)}}$
$\Delta_7 = \frac{(g_1^{(p)})^2}{2}, \frac{1+(g_1^{(p)})^2}{2}, \frac{(g_2^{(p)})^2}{2}, \frac{1+(g_2^{(p)})^2}{2}, \frac{\alpha_1^{(p)}}{2}, \frac{1+\alpha_1^{(p)}}{2}, \frac{\alpha_2^{(p)}}{2}, \frac{1+\alpha_2^{(p)}}{2}, \frac{d_1^{(p)}}{2}, \frac{1+d_1^{(p)}}{2}, \frac{d_2^{(p)}}{2}, \frac{1+d_2^{(p)}}{2},$ $\{\frac{v_1^{(p)}}{2}\}_1^{k_1^{(p)}}, \{\frac{1+v_1^{(p)}}{2}\}_1^{k_1^{(p)}}, \{\frac{v_2^{(p)}}{2}\}_1^{k_2^{(p)}}, \{\frac{1+v_2^{(p)}}{2}\}_1^{k_2^{(p)}}, 0, 0$
$\Delta_8 = \frac{1-\lambda_1^{(p)}}{2}, \frac{2-\lambda_1^{(p)}}{2}, \frac{1-\lambda_2^{(p)}}{2}, \frac{2-\lambda_2^{(p)}}{2}, 0, 1, \frac{1+(g_1^{(p)})^2}{2}, \frac{2+(g_1^{(p)})^2}{2}, \frac{1+(g_2^{(p)})^2}{2}, \frac{2+(g_2^{(p)})^2}{2},$ $\{\frac{1+v_1^{(p)}}{2}\}_1^{k_1^{(p)}}, \{\frac{2+v_1^{(p)}}{2}\}_1^{k_1^{(p)}}, \{\frac{1+v_2^{(p)}}{2}\}_1^{k_2^{(p)}}, \{\frac{2+v_2^{(p)}}{2}\}_1^{k_2^{(p)}}$

Flow chart of Monte-Carlo simulations

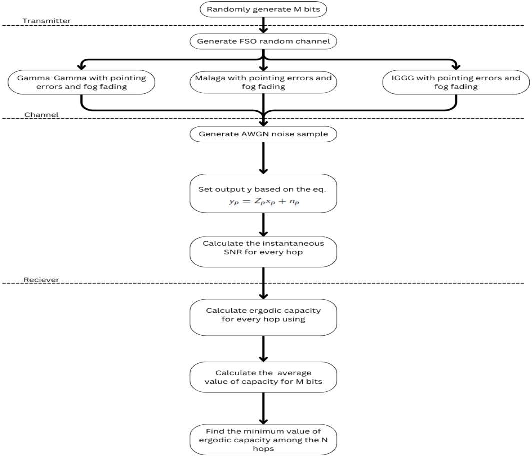

Fig. 2: Flow chart of Monte-Carlo simulations

Multihop ORS-Assisted FSO: Simulation Parameters

Table 4: Simulation Parameters

Parameter	Values
Shape parameter of fog, $k^{(p)}$	2
Scale parameter of fog, $\psi^{(p)}$	13.12
Pointing error coefficient, $g^{(p)}$	2.7
Link distance (Tx to IRS), L_1	1000 m
Link distance (IRS to Rx), L_2	1000 m
No. of hops, N	3
No. of IRS elements, M	1

Multihop ORS-Assisted FSO: Numerical Results

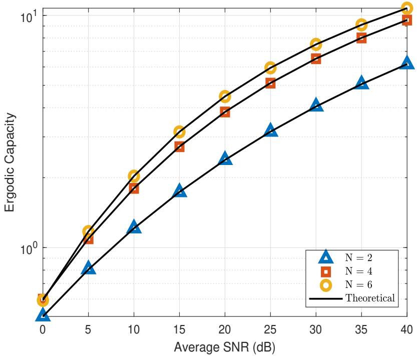

Fig. 3: Ergodic capacity for different no. of hops (Gamma-Gamma)

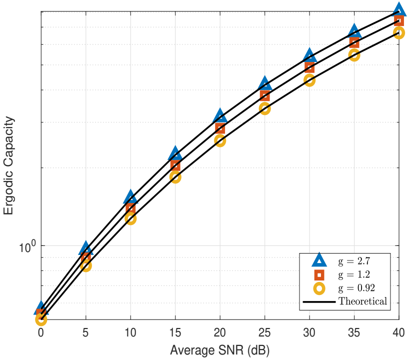

Fig. 4: Ergodic capacity for different values of pointing error coefficient (Málaga)

- To achieve a capacity of 3 bits/sec/Hz, $N = 6$ has an SNR gain of 5 dB and 12 dB while compared to $N = 4$ and $N = 2$, respectively
- As the number of hops increases, the atmospheric severity will decrease, due to which the capacity value increases
- As the pointing error coefficient decreases, capacity also decreases

Multihop ORS-Assisted FSO: Numerical Results

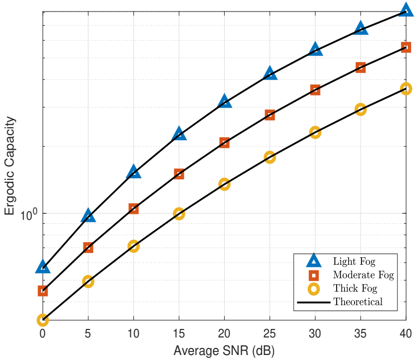

Fig. 5: Ergodic capacity for different different foggy weather conditions (IGGG)

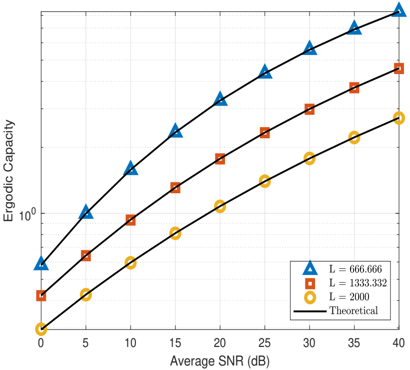

Fig. 6: Ergodic capacity for different link distance (Gamma-Gamma)

- As the severity of fog increases, capacity decreases
- An increase in the link distance decreases the capacity as atmospheric turbulence severity will increase (i.e., α_i, β_i values will decrease)

Multihop ORS-Assisted FSO: Numerical Results

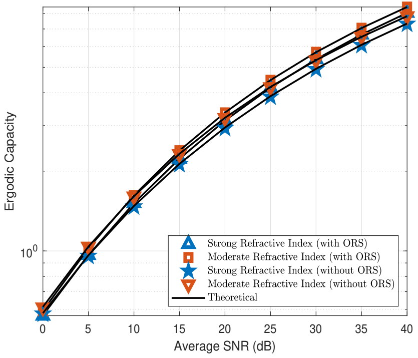

Fig. 7: Ergodic capacity for different refractive index values (Malaga)

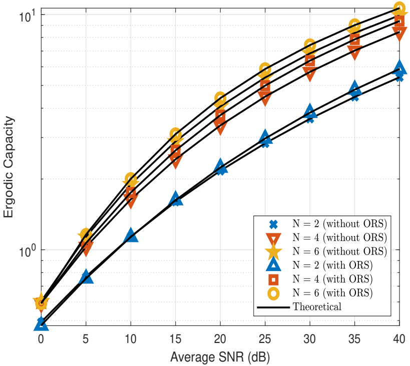

Fig. 8: Comparision between ergodic capacity of the system with and without IRS (IGGG)

- The minimum capacity requirement of the eMBB usage scenario in a 5G system is achieved at an SNR of 25 dB with ORS, but without ORS it is achieved at an SNR of 28 dB
- As the refractive index value increases, atmospheric turbulence severity will increase, and the capacity will decrease
- With the ORS, the system's performance will improve compared to the system without the ORS

Multihop ORS-Assisted FSO: Numerical Results

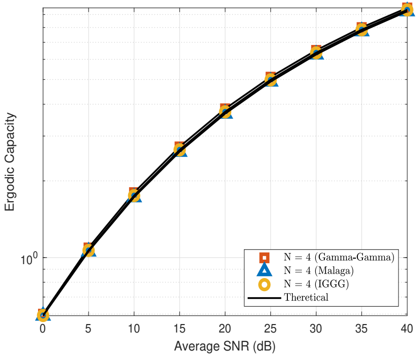

Fig. 9: Comparision between Gamma-Gamma, Málaga, and IGGG distributions

- When $\lambda_i \to \infty$ (i.e., $\lambda_i \geq 13$), IGGG reduces to the GG turbulence model, while all other parameters remain unchanged
- Similarly for $\rho = 1$, $\Omega' = 1$, and $Y = 0$, Málaga reduces to Gamma-Gamma model
- As a special case, IGGG, and Málaga reduce to the Gamma-Gamma model

Conclusions

- This work described the Multihop ORS-assisted FSO system under the effect of fog, AT, and pointing errors
- To model atmospheric turbulence, we have considered GG, IGGG, and Màlaga distribution
- Closed-form EC expressions for different AT turbulence models were derived and validated using Monte-Carlo simulations
- While increasing the pointing error severity, the performance of the system decreases
- With an increase in the intensity of fog, the performance decreases, this is due to varying degrees of attenuation, scattering, and absorption of optical signals
- The capacity performance of various AT turbulence models has been compared and observed that the performance of different models is nearly the same. IGGG and Màlaga distribution will be reduced to GG as a special case
- The Multihop ORS-assisted FSO system offered improved performance as compared to the single-hop ORS-assisted FSO system and Multihop FSO system without ORS

Future Works

- To obtain an asymptotic capacity expression for the given system model
- We will extend our work to multi-hop N IRS element FSO communication system
- The model discussed assumes perfect CSI conditions both at the ORS as well as at the receiver; imperfect CSI can be explored as a part of future work.
- For the ORS, perfect phase cancellation in order to maximize the SNR is assumed, as a part of the future work the non-ideal conditions for example non-unity ORS reflection coefficient and imperfect phase cancellation at ORS can be considered.

References

[1] E. Zedini, H. Soury, and M.-S. Alouini, “Dual-hop FSO transmission systems over gamma-gamma turbulence with pointing errors,” IEEE Trans. Wireless Commun. 16, 784–796 (2017).
[2] E. Zedini, H. Soury, and M.-S. Alouini, “On the performance analysis of dual-hop mixed FSO/RF systems,” IEEE Trans. Wireless Commun.15, 3679–3689 (2016).
[3] T. A. Tsiftsis, H. G. Sandalidis, G. K. Karagiannidis, and N. C. Sagias, “Multihop free-space optical communications over strong turbulence channels,” in IEEE International Conference on Communications (2006), Vol. 6, pp. 2755–2759.
[4] L. Yang, W. Guo, and I. S. Ansari, “Mixed dual-hop FSO-RF communication systems through reconfigurable intelligent surface,” IEEE Commun. Lett. 24, 1558–1562 (2020).
[5] Smriti Uniyal, Narendra Viswakarma, and R. Swaminathan, "Multihop IRS-assisted free space optics communication with DF relaying: a performance analysis," J. Opt. Commun. Netw. 62, 4716-4726 (2023).
[6] Deepshikha Singh and Swaminathan R, "Comprehensive Performance Analysis of Hovering UAV-Based FSO Communication System," IEEE Photon.J., vol. 14, no. 5 (2022).
[7] P. Sharma, R. Swaminathan, and D. Singh, “Multi-hop UAV-based FSO system over doubly inverted gamma-gamma turbulence channel,” IEEE Commun.Lett., vol.28, no.10, pp. 2313–2317 (2024).
[8] S. S. Ikki and S. Aissa, “Multihop wireless relaying systems in the presence of cochannel interferences: Performance analysis and design optimization,” IEEE Trans.Veh.Technol., vol. 61, no. 2, pp. 566–573 (2012).

Thank You